

## TWO-PHASE HEAT TRANSFER AND PRESSURE LOSSES OF A HIGH PRESSURE REFRIGERANT CONDENSING IN A SINGLE CIRCULAR MINICHANNEL

A. Cavallini\*, S. Bortolin, D. Del Col, M. Matkovic, L. Rossetto

\*Author for correspondence

Dipartimento di Fisica Tecnica, University of Padova,

Via Venezia 1, I-35131 Padova, Italy

Tel. +39 049 8276890 – Fax +39 049 8276896 – Email: alcav@unipd.it

### ABSTRACT

A 0.96 mm circular minichannel is used to measure both two-phase pressure losses and heat transfer during condensation of the high pressure refrigerant R32.

The test runs have been performed during condensation at around 40°C saturation temperature, corresponding to 24.8 bar saturation pressure. The pressure drop tests have been performed in adiabatic flow conditions, to only measure the pressure losses due to friction.

The experimental data are compared against predicting models both for condensation heat transfer and two-phase flow pressure drop inside minichannels.

### INTRODUCTION

A significant and still growing part of the engineering research community has been devoted in the last few decades to scaling down devices, while keeping or even increasing their functionality. The introduction of minichannels in the field of enhanced heat and mass transfer is surely one of those attempts. As a result, compact heat exchangers and heat pipes can be found in a wide variety of applications: from residential air-conditioning to the spacecraft thermal control. Growing interest for different solutions can be also found in electronic cooling, though these applications are less interesting from the condensation point of view due to its exothermal nature. Compact elements work with reduced refrigerant charge and can usually withstand extremely high system pressures.

Two-phase flow in rough minichannels is affected by gravity, inertia, viscous shear and surface tension. These forces influence flow regimes, pressure drops and heat transfer.

Some researchers observed flow regimes during condensation of R134a in minichannels, but no general flow regime map is available. For instance, Coleman and Garimella (2000) reported flow patterns of R134a condensing in horizontal tubes and square minichannels with inner hydraulic diameters ranging from 1 to 4.9 mm. At mass velocities  $G > 150 \text{ kg m}^{-2} \text{ s}^{-1}$  the authors observed annular, wavy, intermittent

(slug, plug) and dispersed (bubble) flow patterns. At hydraulic diameters  $D_h < 1 \text{ mm}$  the wavy regime was not present while at high flow rates and qualities annular film with mist core or mist flows were present. While the hydraulic diameter was found to have a substantial effect on flow transitions, tube shape was found to be less significant. Several other authors have performed visualisations in minichannels, as reported in Cavallini et al. (2008), but no specific visualisation with high pressure fluids has been done.

With regard to the pressure drop behaviour of minichannels, very few data are available in the open literature regarding high pressure fluids. Most data in fact refer to low and medium pressure refrigerants, such as R134a.

Cavallini et al. (2005) measured pressure drops during adiabatic flow at 40 °C of R410A, R134a and R236ea inside a multi-port minichannel having a square cross section with hydraulic diameter 1.4 mm, length 1.13 m and with mass velocities ranging from 200 to 1400  $\text{kg m}^{-2}\text{s}^{-1}$ . The multiport minichannel tested is characterized by a square cross section and a low value of surface roughness ( $Ra = 0.08 \text{ }\mu\text{m}$  and  $Rz = 0.43 \text{ }\mu\text{m}$ ), whose effect can thus be neglected.

The authors compared their data against models, either developed for conventional macrochannels or specifically developed for minichannels. No model was able to predict frictional pressure drops of R410A, while many models were not able to predict R236ea trends. Better predictions, however, were obtained for the frictional pressure drops of R134a.

A new model for the frictional pressure gradient valid for adiabatic flow or for flow during condensation of halogenated refrigerants inside minichannels was then suggested by Cavallini et al. (2008). The model was first suggested for smooth tubes since it is based on data taken in channels with negligible surface roughness and takes into account the effect of the entrainment rate of droplets from the liquid film. This model can be applied to the annular, annular-mist and intermittent flows and can also be applied with success to

horizontal macro tubes. This same model has been also modified to account for roughness in minichannels.

As to visualization and pressure drop, most of the heat transfer data available in the literature for condensation inside minichannels were taken with the fluid R134a and in most cases multiport channels have been used. In multiport tubes, averaged values over a number of parallel channels are measured instead of the heat transfer coefficient in one single channel.

Actually it is not an easy task to perform local heat transfer coefficient measurements during condensation inside a single minichannel and it may be more complicated as compared to the flow boiling case, where electrical heating can be adopted. In this context, a new experimental apparatus for the measurement of the local heat transfer coefficients inside the single minichannel has been recently set up at the University of Padova. On this apparatus, condensation tests have been performed in a 0.96 mm diameter circular channel.

The fluid investigated in this paper, R32, is a so-called high pressure fluid, displaying higher vapour density as compared to R134a. In practical applications, the use of a high pressure refrigerant can mitigate the disadvantage of the higher pressure drop due to the smaller channel diameter. R32 also displays high thermal conductivity, which is favorable to high heat transfer coefficients during condensation.

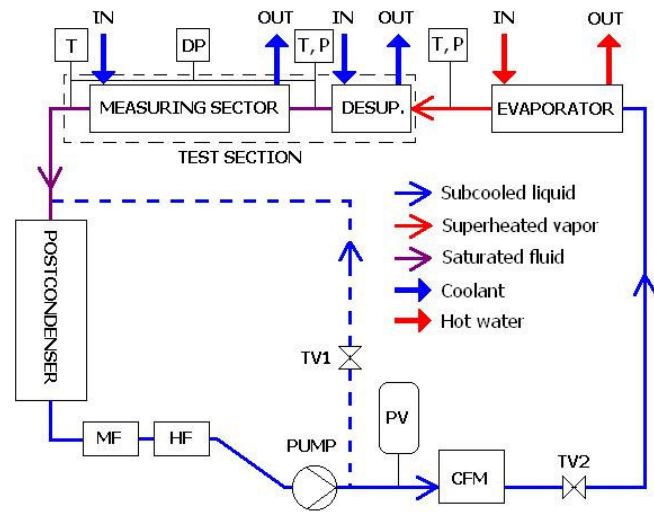


Figure 1 Experimental test rig: DESUP.=desuperheater, MF=mechanical filter, HF=drier, PV=pressure vessel, CFM=Coriolis-effect mass flow meter, P=pressure transducer, T=temperature transducer, DP=differential pressure transducer.

## NOMENCLATURE

|          |                                       |                            |
|----------|---------------------------------------|----------------------------|
| $c_{pw}$ | [J kg <sup>-1</sup> K <sup>-1</sup> ] | specific heat of water     |
| $D$      | [m]                                   | tube inside diameter       |
| $f$      | [-]                                   | friction factor            |
| $g$      | [m s <sup>-2</sup> ]                  | gravitational acceleration |
| $G$      | [kg m <sup>-2</sup> s <sup>-1</sup> ] | mass velocity              |
| $h_{LG}$ | [J kg <sup>-1</sup> ]                 | heat of vaporization       |

|           |                                      |  |
|-----------|--------------------------------------|--|
| $HTC$     | [W m <sup>-2</sup> K <sup>-1</sup> ] | heat transfer coefficient  |
| $m$       | [kg s <sup>-1</sup> ]                | mass flow rate   |
| $p$       | [Pa]                                 | pressure   |
| $Ra$      | [μm]                                 | arithmetical mean deviation of the assessed profile (according to ISO 4287 : 1997) |
| $Re_{LO}$ | [-]                                  | = $G D_h / \mu_L$  |
| $Rr$      | [-]                                  | relative roughness of the tube   |
| $Rz$      | [μm]                                 | maximum height of profile (according to ISO 4287 : 1997)                           |
| $x$       | [-]                                  | thermodynamic vapor mass quality   |
| $z$       | [m]                                  | axial coordinate oriented with the flow  |

|                    |     |                                     |
|--------------------|-----|-------------------------------------|
| Special characters |     |                                     |
| $\delta$           | [m] | liquid film thickness               |
| $\delta^*$         | [-] | dimensionless liquid film thickness |
| $\Delta$           | [-] | variation                           |

|            |  |
|------------|--|
| Subscripts |  |
| $CALC$     | calculated                             |
| $EXP$      | experimental                           |
| $f$        | frictional                             |
| $h$        | hydraulic                              |
| IN         | at the inlet                           |
| LO         | liquid phase with total mass flow rate |
| TC, TP     | thermocouple, thermopile               |
| r, c       | refrigerant, coolant                   |
| MS, PS     | measuring sector, pre-sector           |

## PRESSURE DROP TESTS IN A ROUGH SINGLE MINICHANNEL

The present authors report here the pressure drop measured during adiabatic two-phase flow of R32. The mini-tube used displays a much higher surface roughness as compared to the previously tested multiport minichannels (Cavallini et al., 2005) and this allows to investigate the effect of tube wall roughness of the channel on the two-phase frictional pressure gradient. In fact, as shown by Taylor et al. (2006), surface roughness affects pressure drop during single phase flow in macrochannels and minichannels.

Some single phase flow tests have previously been performed with R134a to measure the friction factor in the minichannel. Experimental values of R134a friction factor have been compared against equations for both laminar flow and turbulent flow in rough tubes and a good agreement between calculated and experimental values was found.

In order to consider the effect of the tube wall roughness, the all liquid friction factor of the Cavallini et al. (2006) model was corrected in the following way:

$$f_{LO} = 0.046 Re_{LO}^{-0.2} + 0.7 \cdot Rr \quad \text{for } Rr < 0.0027$$

The above friction factor is in good agreement with the Churchill (1977) curve in the range  $3000 < Re_{LO} < 6000$ .

The test rig arranged for heat transfer and pressure drop measurements during condensation is depicted in Fig.1. It consists of the primary refrigerant loop and four auxiliary loops. The subcooled refrigerant is sent through a filter and a drier into the gear pump coupled with a variable speed electric motor. It is then pumped through the Coriolis-effect mass flow meter into the evaporator where the fluid is heated up, vaporized and superheated. There, the temperature and the pressure define the state of the superheated vapour.

The superheated vapour enters the test section, which is composed of two counter current heat exchangers. The first one (desuperheater) is used to cool down the fluid to the saturation state at the inlet of the second heat exchanger, which is the actual measuring sector.

Some frictional tests have been performed at low vapour quality; in this case it is possible to bypass the evaporator and to send the refrigerant to the test section as subcooled liquid and to use the desuperheater as a preheater for the liquid. Indeed, saturation conditions are achieved by partial vaporisation before the measuring sector.

The saturation temperature is checked against pressure in the two adiabatic sectors upstream and downstream of the measuring sector. There, the temperature is detected by means of adiabatic wall temperature measurements. Saturated refrigerant enters the measuring sector, where the measurement is performed. The refrigerant state is finally checked at the outlet of the measuring sector and the loop is closed in the postcondenser, where it is condensed and subcooled. The temperatures and the flow rates of the secondary loops are controlled by a closed hot water loop, two thermal baths and an additional resistance heater set in series at the inlet of the desuperheater. In this way, it is possible to independently control the temperatures of four different heat sinks or heat sources within the test rig.

The test tube is a commercial copper tube with inner diameter 0.96 mm and 228.5 mm length. The arithmetical mean deviation of the assessed profile  $Ra$  of the inner surface is  $Ra=1.3 \mu\text{m}$ , the maximum height of profile  $Rz$  is  $10 \mu\text{m}$ . The inlet and outlet pressure ports are inserted in two stainless steel tubes 24 mm attached to the ends of the copper tube. The stainless steel tubes have 0.762 mm inner diameter,  $Ra = 2.0 \mu\text{m}$  and  $Rz = 10.2 \mu\text{m}$ . The total frictional pressure drop is then the sum of the frictional pressure drop in the two stainless steel tubes, each 24 mm long, of the frictional pressure drop in the 228.5 mm long copper tube and of the pressure variations due to one abrupt enlargement (from 0.762 mm diameter to 0.96 mm diameter) and one contraction (from 0.96 mm to 0.762 mm).

The experimental uncertainty for the measured pressure difference is  $\pm 0.1 \text{ kPa}$ , for the absolute pressure is  $\pm 3 \text{ kPa}$ , for the refrigerant flow rate is  $\pm 0.2\%$ , for the vapor quality  $\pm 1\%$ .

Adiabatic two-phase pressure drop tests have been performed during R32 flow in the same test section as described above. Inlet vapor quality has been controlled through the thermal balance in the desuperheater. It has been used for partial condensation of the superheated vapor or for partial vaporization of the subcooled refrigerant at the inlet of the test section. Figure 2 shows the total experimental pressure drop for R32 at  $40^\circ\text{C}$  versus vapor quality, at 200, 400, 600, 800 and  $1000 \text{ kg m}^{-2} \text{ s}^{-1}$  mass velocities.

Figure 2 and Figure 3 show the comparison between the experimental  $\Delta p_{total}$  data and the calculated values with the Cavallini et al. (2008) model for linear losses and according to Paliwoda (1992) for abrupt geometry changes. The present model shows an excellent agreement with data.

In order to enlighten the effect of the roughness in the minichannel, one can calculate the liquid film thickness  $\delta$  at the

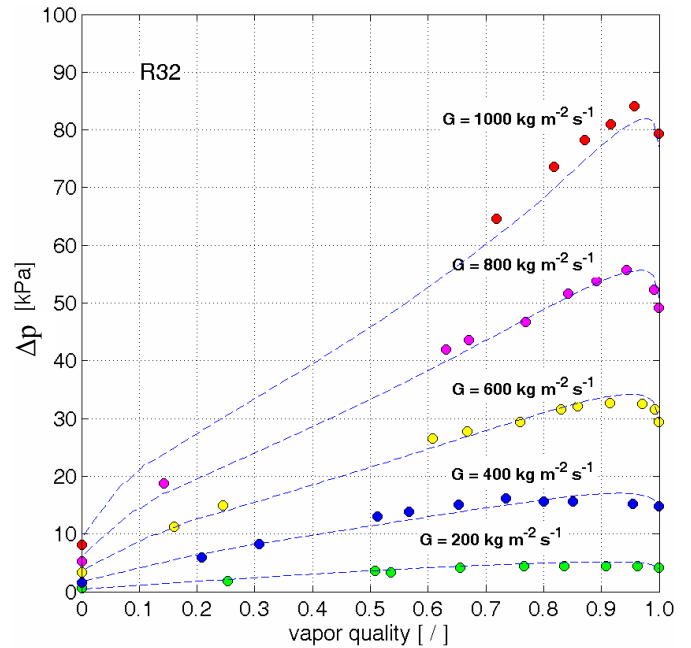


Figure 2. Cumulative experimental pressure drop in the test channel during adiabatic two-phase flow of R32 and calculated trends. Paliwoda (1992) has been used for local pressure drops while Cavallini et al. (2008) has been used for frictional pressure losses calculation.

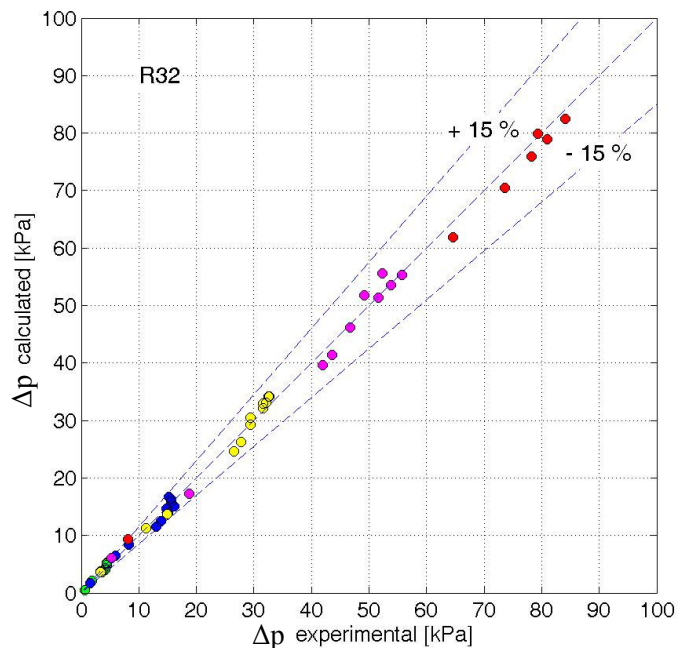


Figure 3. Calculated versus experimental pressure drop of R32 (using models by Paliwoda 1992 and Cavallini et al., 2008).

wall by using the model by Cavallini et al. (2006b) for condensation in minichannels during annular flow, based on the Kosky and Staub (1971) analysis for macrochannels.

For experimental data at high vapour qualities ( $x > 0.7$ ), the dimensionless film thickness  $\delta^+$  is around 18 at mass velocity between 400 and  $800 \text{ kg m}^{-2} \text{ s}^{-1}$ , which means that the liquid

film is laminar near the wall and in the transition to turbulent flow away from the wall. It corresponds to a liquid film  $\delta$  at the wall between 11 and 19  $\mu\text{m}$  (with lower film thickness at higher mass velocity). Therefore, the surface roughness, with peaks up to 15  $\mu\text{m}$  high, certainly affects the laminar and the laminar-turbulent transition sublayers. The liquid flow is influenced by both vapor shear stress and surface roughness. It should also be considered that the laminar sublayer is characterized by an even lower thickness.

When the peak height is larger than the liquid film thickness, the liquid film may also be influenced by the surface tension at the peaks and in the valleys between the peaks.

### CONDENSATION TESTS

In order to investigate heat transfer within a single minichannel a unique measuring test section has been designed (Figure 4) and built (Matkovic et al., 2008). Either single-phase tests or experiments during forced convective condensation and flow boiling can be studied with the present facility. The test section is made of a straight single minichannel with two diabatic and two adiabatic sectors along its length. The diabatic sectors work as heat exchangers with the presence of a secondary fluid, which is water. The two sectors are made from an 8 mm external diameter copper rod with a 0.96 mm internal bore which is the minichannel itself. The thick-walled tube was machined externally so as to obtain a cooling water channel within the wall thickness. The tortuous path for the secondary fluid, surrounded with plastic sheath, enables a good water mixing and thus allows precise local coolant temperature measurements. In this test section, 15 thermocouples have been inserted into the water channel along the MS in order to measure the coolant temperature profile. The enhanced coolant heat transfer surface area moves the thermal resistance toward the internal side and thus reduces the experimental heat transfer coefficient error due to the refrigerant to wall temperature difference.

In order to measure precise local HTC values 15 thermocouples have been inserted into the wall thickness, near the minichannel along the measuring sector, without having the thermocouple wires cross the coolant path. Furthermore, two single thermocouples and one thermopile are measuring the refrigerant temperature by measuring the external wall surface temperature of the adiabatic sectors – stainless steel capillary tubes at the two extremes of the measuring sector. When

operating in condensation mode, the first diabatic sector works as a desuperheater. To avoid big temperature gradients at the inlet of the measuring sector the desuperheater is used to cool down the superheated refrigerant to the saturation state at the inlet of the measuring sector. Vapor quality is there obtained from the thermal balance on the coolant side, whereas saturation conditions are checked using the adiabatic wall temperature and the pressure measurement in the adiabatic sectors.

The following three parameters are used for the determination of the local heat transfer coefficient: the local heat flux, the saturation temperature and the wall temperature. The heat flux is determined from the temperature profile of the coolant in the measuring sector. The wall temperature is directly measured along the test section and the saturation temperature is measured in the adiabatic segments at the inlet and outlet of the test tube and checked through pressure transducers.

The coolant temperature profile is obtained from the thermocouples set in the water channel along the measuring sector (Figure 5). The derivative of the temperature profile is proportional to the local heat flux:

$$q'(z) = -\dot{m}_c \cdot c_{pw} \frac{1}{\pi \cdot d_i} \cdot \frac{dT_c(z)}{dz}$$

and it is associated to the local heat transfer coefficient:

$$HTC_i(z) = \frac{q'(z)}{(T_{sat}(z) - T_{wall}(z))}$$

The local saturation temperature ( $T_{sat}(z)$ ) of the fluid along the sector is calculated from the two measured values in the adiabatic sectors. The calculation, which considers frictional pressure drop and pressure recovery due to condensation, is iterative. It is modified so as to take into account the local pressure gradient profile and make the saturation temperature curve converge to the saturation temperature measurement at the outlet of the measuring sector. On the other hand, the wall temperature ( $T_{wall}(z)$ ) is measured locally.

By considering the conservation of energy in the sector, the coolant temperature change is directly associated to the corresponding enthalpy variation of the refrigerant. Therefore, the local vapor quality is calculated as follows:

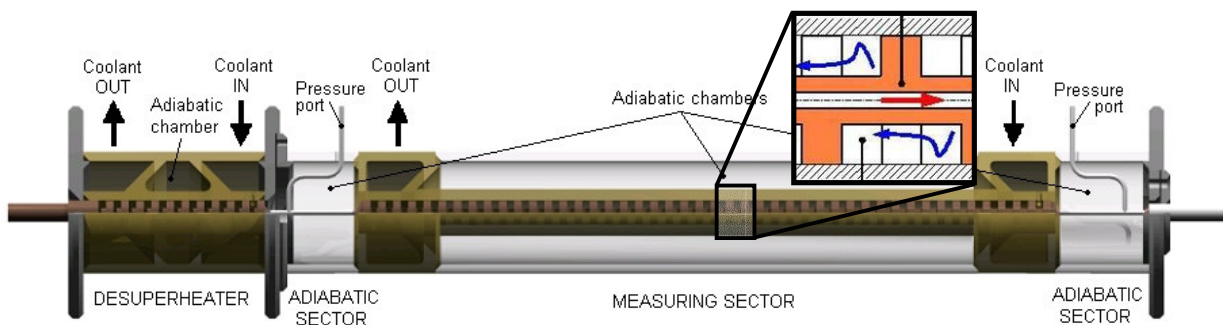


Figure 4: Schematic of the experimental test section.

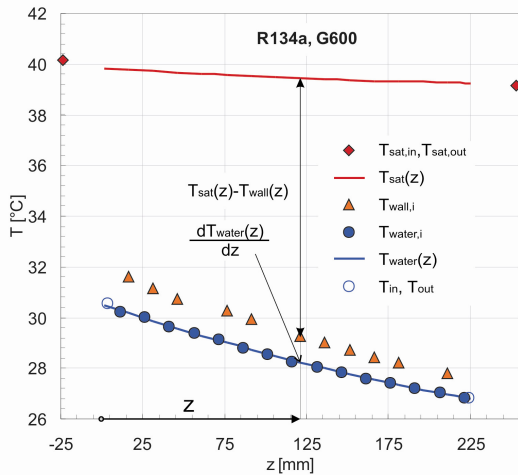


Figure 5. Temperature measurements within the single minichannel test section.

$$x(z) = x_{in} - \frac{\pi \cdot d_i \cdot \int_0^z q'(z) dz}{\dot{m}_r \cdot h_{LG}}$$

The local heat transfer coefficient has been measured during condensation of the high pressure refrigerant R32. The experiments have been performed over the entire range of vapor quality at 40°C saturation temperature and mass velocity ranging from 100 kg m<sup>-2</sup>s<sup>-1</sup> up to 1200 kg m<sup>-2</sup>s<sup>-1</sup>.

The complete set of the experimental heat transfer coefficients is plotted in Figure 6 versus vapor quality. As expected for forced convective condensation inside conventional pipes, the heat transfer coefficient increases with mass velocity and vapor quality. The experimental heat transfer coefficients measured at 100 kg m<sup>-2</sup>s<sup>-1</sup> and those at 200 kg m<sup>-2</sup>s<sup>-1</sup> are very close to each other, showing little effect of mass velocity at these conditions. It is worth reminding that the lower the mass transfer coefficient, the higher the experimental uncertainty of the heat transfer coefficient, due to the low local heat fluxes. Nevertheless, this overlapping of the HTC at the lower tested values of mass velocity was not found with the refrigerant R134a and may be explained with the flow pattern and the properties of R32.

In the present technique, the dominant thermal resistance during the condensing process is on the refrigerant side, as can be seen from Figure 5. This is favorable to the reduction of the experimental uncertainty associated to the determination of the heat transfer coefficient. Since the purpose of the present apparatus is to accurately measure the local heat transfer coefficient, several tests have been performed to verify that the heat transfer coefficient does not depend on the conditions of the secondary fluid.

Besides mass velocity and vapor quality, the effect of the saturation to wall temperature difference can be investigated by varying the inlet temperature of the coolant. Such a study has been conducted at 200 kg m<sup>-2</sup>s<sup>-1</sup> with coolant temperature ranging between 19 and 29 °C, at constant refrigerant saturation temperature. Because of the peculiar design of the coolant channel these variations of the coolant temperature imply a consequent significant change in the wall temperature and thus in the saturation to wall temperature difference. The results are plotted in Figure 7, showing no effect of the temperature difference in the heat transfer coefficient at 200 kg m<sup>-2</sup>s<sup>-1</sup>. These results confirm that, at this mass velocity, the effect of gravity forces in around 1 mm diameter channels is not significant in comparison with the other forces influencing the condensation heat transfer.

Experimental results have been compared against two models available in the open literature and developed for HTC predictions inside macro-scale tubes: Moser et al. (1998) and Cavallini et al. (2006a). The model by Moser et al. (1998), which was initially developed for conventional pipes and later on modified by using the Zhang and Webb (2001) method for pressure drop calculation inside small-diameter tubes, can be applied only to annular flow condensation, whereas the model by Cavallini et al. (2006a) also accounts for the transition from annular to stratified flow at low mass velocity.

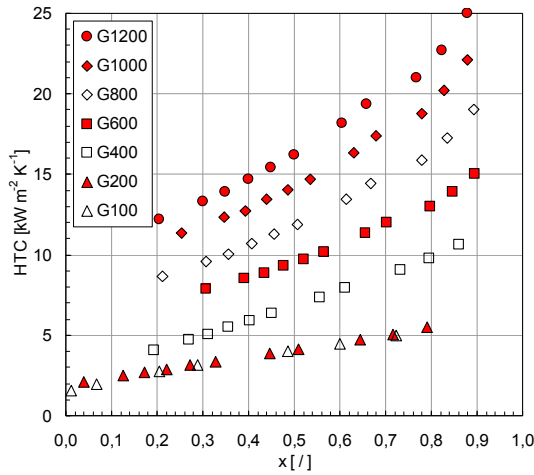


Figure 6. Heat transfer coefficient measured during condensation of R32 in the channel versus vapor quality.

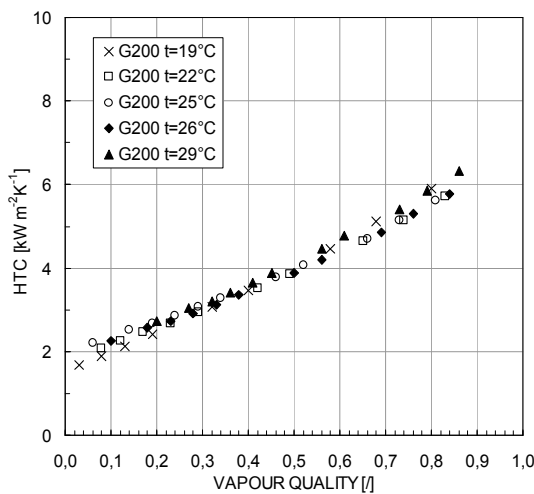


Figure 7. Experimental heat transfer coefficient during condensation of R32 at different inlet coolant temperature.

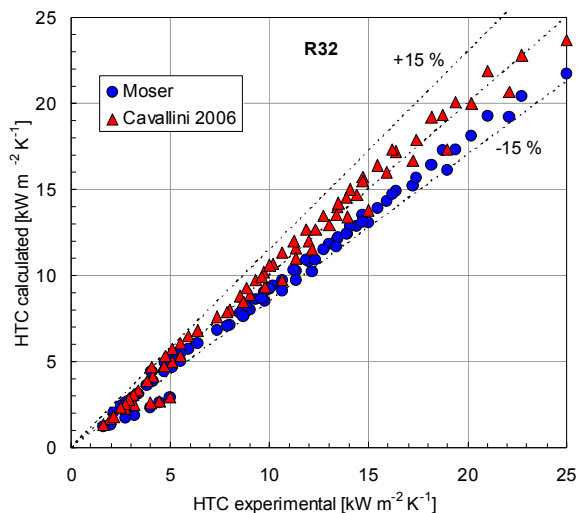


Figure 8. Calculated versus experimental heat transfer coefficient: the model by Moser et al. (1998), modified by Zhang and Webb (2001) and the model by Cavallini et al. (2006a) are applied.

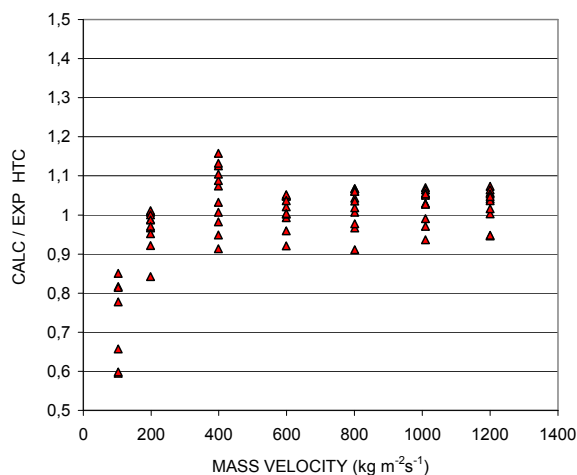


Figure 9. Ratio of calculated to experimental heat transfer coefficient versus mass velocity: the model by Cavallini et al. (2006a) is applied.

The graph in Figure 8 shows the good performance of these models developed for macro-scale condensation. The only data points which are not accurately predicted are the ones measured at  $100 \text{ kg m}^{-2}\text{s}^{-1}$ . This is clearly shown in Figure 9 where the ratio of calculated to experimental heat transfer coefficient is plotted versus mass velocity and the model by Cavallini et al. (2006a) is applied. At mass velocity higher or equal to  $200 \text{ kg m}^{-2}\text{s}^{-1}$ , where the condensation heat transfer is likely to be dominated by shear stress, the macroscale model can accurately predict the heat transfer coefficient. At lower mass velocity, the agreement is not sufficiently accurate; that means that the computation procedure based on macroscale condensation data is not applicable at these low flow rates.

## CONCLUSIONS

In this paper, two-phase frictional pressure drops and condensation heat transfer coefficients measured with R32 in a  $0.96 \text{ mm}$  diameter single round channel have been reported.

The experimental pressure drops have led to the conclusion that the surface roughness affects the motion of the liquid film. The present data can be accurately predicted by accounting for the surface roughness in the computation of the single phase friction factor.

The experimental values of the heat transfer coefficient show that the condensation is shear stress dominated for most of the data points and in this range of operating conditions they can be well predicted by using the Cavallini et al. (2006a) model for macroscale condensation.

## REFERENCES

- Cavallini A., Censi G., Del Col D., Doretti L., Matkovic M., Rossetto L. and Zilio C., 2006a, Condensation in Horizontal Smooth Tubes: A New Heat Transfer Model for Heat Exchanger Design. *Heat Transfer Engineering*. Vol. 27 no.8, pp. 31-38.
- Cavallini, A., Del Col, D., Doretti, L., Matkovic, M., Rossetto, L., and Zilio, C., 2005, "Two-phase frictional pressure gradient of R236ea, R134a and R410A inside multi-port mini-channels", *Experimental Thermal and Fluid Science*, 29(7), pp. 861-870.
- Cavallini, A., Del Col, D., Matkovic, M., Rossetto, L., 2008, "Frictional pressure drop during vapor-liquid flow in minichannels: modelling and experimental evaluation", Submitted to *Int. J. of Heat and Fluid Flow*.
- Cavallini, A., Doretti, L., Matkovic, M. and Rossetto, L., 2006b, "Update on condensation heat transfer and pressure drop in minichannels," *Heat Transfer Eng.*, 27(4), pp. 74-87.
- Churchill, S.W., 1977, "Friction factor equation spans all fluid-flow regimes", *Chemical Engineering* 45, pp. 91-92.
- Coleman, J.W., and Garimella, S., 2000, "Visualization of refrigerant two-phase flow during condensation", Proc. of the NHTC'00, NHTC2000-12115, ASME, New York.
- Kosky, P. G., and Staub, F. W., 1971, "Local Condensing Heat Transfer Coefficients in the Annular Flow Regime", *AIChE J.*, 17(5), pp. 1037-1043.
- Matkovic M., Cavallini, A., Del Col, D., and Rossetto, L. 2008, "Experimental condensation inside minichannels", submitted to *Int. J. of Heat and Mass Transfer*.
- Moser K. W., Webb R. L., Na B., 1998, A new equivalent Reynolds number model for condensation in smooth tubes, *J. of Heat Transfer*, 120: 410-417.
- Paliwoda, A., 1992, "Generalized method of pressure drop calculation across pipe components containing two-phase flow of refrigerants", *Rev. Int. Froid*, 15(2), pp. 119-125.
- Taylor J.B., Carrano A.L., and Kandlikar S.G., 2006, "Characterization of the effect of surface roughness and texture on fluid flow-past, present, and future", *International Journal of Thermal Sciences*, 45(10), pp. 962-968.
- Zhang, M., and Webb, R.L., 2001, "Correlation of two-phase friction for refrigerants in small-diameter tubes", *Experimental Thermal and Fluid Science*, 25(3-4), pp. 131-139.